

## Synthetic Methods | Hot Paper |

Christina M. Bock,<sup>[a]</sup> Gangajji Parameshwarappa,<sup>[a]</sup> Simon Bönisch,<sup>[b]</sup> Christian Neiss,<sup>[b]</sup> Walter Bauer,<sup>[a]</sup> Frank Hampel,<sup>[a]</sup> Andreas Görling,<sup>\*,[b]</sup> and Svetlana B. Tsogoeva<sup>\*,[a]</sup>

Dedicated to Professor Lutz F. Tietze

**Abstract:** Aza- and carbobicyclic compounds possess favorable pharmaceutical properties, but they are difficult to access. Herein, we demonstrate an unprecedented organo-catalytic two component six-step chemodivergent domino reaction, which provides a straightforward, sustainable and atom economical route to difficult-to-access complex bicyclic architectures: azabicycles and carbobicycles, whose ratios can be controlled by the applied electrophiles and catalysts. Detailed NMR and X-ray studies on the structures and

relative stereochemistry of selected compounds are presented. Mechanistic investigations of the chemoselective branching step have been carried out with DFT methods in conjunction with semiempirical van der Waals interactions. This new domino reaction opens up a new vista of generating, in a single operation, new bioactive compounds with strong antiviral properties (EC<sub>50</sub> up to 0.071 μM for human cytomegalovirus (HCMV)) outperforming clinically used ganciclovir (EC<sub>50</sub> 2.6 μM).

## Introduction

Chemists strive to build complex molecules from simple precursors. Facile preparation of such intricate molecular architectures, like heterobicyclic or carbobicyclic systems, which are otherwise difficult to access by traditional methods, is still a challenge. These compounds are known to play a vital role in drug synthesis. Azabicyclic compounds, among them isoquinuclidine (2-azabicyclo[2.2.2]octane (A)) ring systems (Figure 1), are of eminent importance because of their potential as bioactive compounds or pharmaceuticals<sup>[1]</sup> and as subunits of alkaloid natural products such as ibogaine,<sup>[2]</sup> dioscorine,<sup>[3]</sup> and coronaridine.<sup>[4]</sup> There are also numerous natural compounds (terpenes and alkaloids) and drugs that contain purely carbocyclic scaffolds.<sup>[5]</sup>

Particularly, derivatives of several bridged carbobicyclic compounds with an exocyclic imine group (bicyclo[2.2.2]octan-2-imine (B)) were reported as being highly active against *Trypanosoma b. rhodesiense* and the resistant K1 strain of *Plasmodium falciparum* (Figure 1).<sup>[6]</sup>

Routes by which isoquinuclidine and its derivatives are obtained are still few. Formation of the nitrogen-heterocycle scaffolds (2-azabicyclo[2.2.2]octa-2,5-dienes) has been achieved by dimerization of alkylidenemalononitriles or by related reactions employing CH<sub>3</sub>ONa, KF/Al<sub>2</sub>O<sub>3</sub>, K<sub>2</sub>CO<sub>3</sub>/Al<sub>2</sub>O<sub>3</sub>, and [In(OTf)<sub>3</sub>]/Et<sub>3</sub>N as catalysts.<sup>[7]</sup> Azabicycles have also been successfully obtained by Mannich-aza-Michael reactions using a chiral phosphoric Brønsted acid catalyst<sup>[8]</sup> and a proline-derived catalyst.<sup>[9]</sup> Diels-Alder reactions of 1,2-dihydropyridines with dienophiles are also known to provide isoquinuclidine derivatives.<sup>[10]</sup>

Synthetic routes to bridged carbobicyclic compounds are also quite rare and usually involve Diels-Alder reactions with cyclohexa-1,3-dienes<sup>[11]</sup> or tandem Michael additions with deprotonated cyclohexenones.<sup>[12]</sup>

Some practical shortcomings of the previously reported synthetic methodologies<sup>[7-12]</sup> towards azabicycles and carbobicycles include the requirement of cyclic starting materials (which are either unstable (e.g., 1,2-dihydropyridines) or not readily available (e.g., cyclohexa-1,3-dienes), the requirement of isolation of product intermediates in most cases, and/or the requirement of metal-based catalysts.

Interestingly, this reaction, which enables a convenient direct and metal-free route to complex bridged carbo- and heterobicycles using malononitrile and aldehyde as strikingly simple starting compounds, has never been investigated

[a] C. M. Bock, Dr. G. Parameshwarappa, Prof. Dr. W. Bauer, Dr. F. Hampel, Prof. Dr. S. B. Tsogoeva  
Institute of Organic Chemistry and  
Interdisciplinary Center for Molecular Materials (ICMM)  
Friedrich-Alexander-Universität Erlangen-Nürnberg  
Henkestrasse 42, 91054, Erlangen (Germany)  
E-mail: svetlana.tsogoeva@fau.de

[b] S. Bönisch, Dr. C. Neiss, Prof. Dr. A. Görling  
Chair of Theoretical Chemistry and  
Interdisciplinary Center for Molecular Materials (ICMM)  
Friedrich-Alexander-Universität Erlangen-Nürnberg  
Egerlandstrasse 3, 91058, Erlangen (Germany)  
E-mail: andreas.goerling@fau.de

Supporting information and ORCID from the author for this article is available on the WWW under <http://dx.doi.org/10.1002/chem.201504798>.

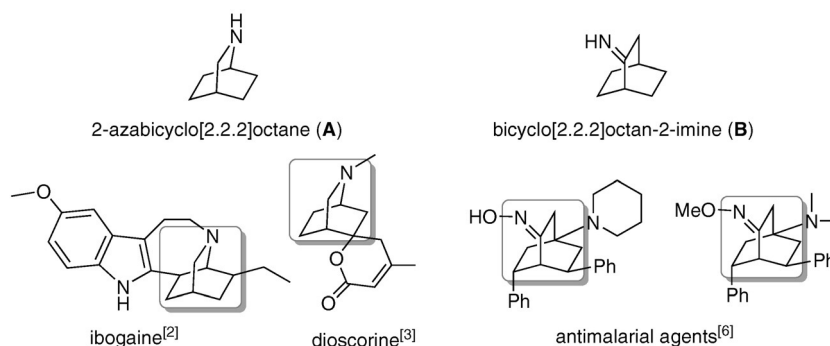


Figure 1. Nitrogen-containing bicyclic structures as subunits of natural products and bioactive compounds.

before. Herein, we report our unexpected discovery of this atom-economical metal-free six-step domino transformation, which employs only two commonly used simple reactants and leads in a single operation to complex compounds like isoquinuclidine derivative **3** and its isomeric carbobicyclic **4** (containing an exocyclic imine group), which are of high value to medicinal chemistry. We have also performed NMR spectroscopy, MS studies, X-ray analysis, and density functional theory (DFT) calculations to elucidate the reaction mechanism and the observed chemoselectivities.

## Results and Discussion

### Development of a new multi-step domino reaction

In 2008, our lab demonstrated the first asymmetric organocatalytic Mannich-type reaction of unmodified ketones with *N*-benzoylhydrazones.<sup>[13]</sup> We recently became interested to extend

the substrate scope of this Mannich-type reaction to malononitrile as a CH-acidic compound. Thus, carrying out this new reaction of phenylethanal-derived *N*-benzoylhydrazone **1** (1 equiv) with malononitrile **2** (1.5 equiv) in the presence of imidazole as a catalyst, we, surprisingly, observed the formation of a mixture of highly substituted isoquinuclidine heterocycle **3a** and its carbobicyclic isomer **4a** in 1:19 ratio with an overall yield of 57% (Figure 2) instead of the expected Mannich-type product.

We hypothesized that the observed products **3a** and **4a** could result from the imidazole-catalyzed reaction of the nucleophilic malononitrile **2** with *N*-benzoylhydrazone **1** by in situ release of *N*-benzoyl-hydrazine group (Figure 2).

Because aldehydes are more electrophilic and more simple starting materials than hydrazones, we decided to use the corresponding aldehyde **5a** in the following experiments. We first carried out the direct reaction of the phenylethanal **5a** (1 equiv) with malononitrile **2** (1.5 equiv) in the presence of an

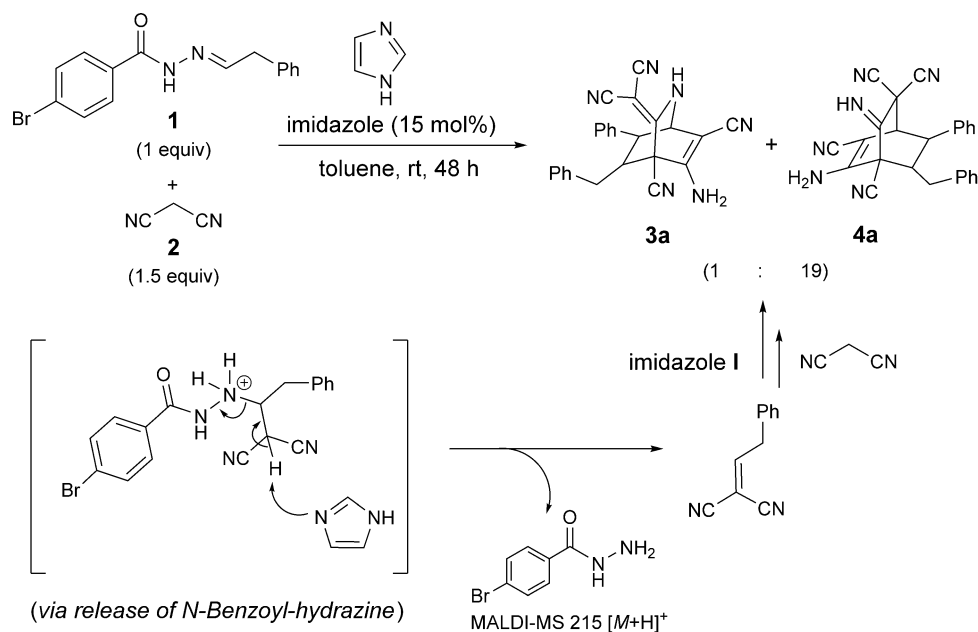
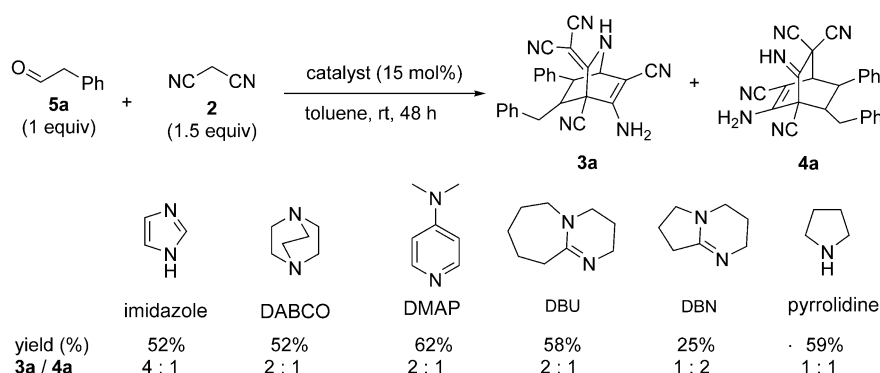


Figure 2. Imidazole-catalyzed formation of isoquinuclidine heterocycle **3a** and its carbobicyclic isomer **4a**.



**Figure 3.** Evaluation of base catalysts for the reaction of phenylethanal **5a** with malononitrile **2**. Reported yields were isolated yields of products (sum of **3a** and **4a**).

imidazole at 15 mol% loading. Interestingly, isoquinuclidine **3a** was formed as the main product in contrast to the reaction employing *N*-benzoylhydrazone **1** as an electrophile. Products **3a** and **4a** were formed in 4:1 ratio with 52% overall yield (Figure 3).

Carrying out the reaction using 1,5-diazabicyclo[4.3.0]non-5-ene (DBN) as a catalyst gave the products in only 25% yield. Generally, higher yields (52–62%) were obtained using diazabicyclo[2.2.2]octane (DABCO), 4-dimethylaminopyridine (DMAP), 1,8-diazabicyclo[5.4.0]undec-7-ene (DBU) and pyrrolidine (Figure 3). However, the chemoselectivity decreased (the ratio of products **3a/4a** ranged from 1:1 to 2:1) compared with that of the imidazole-catalyzed reaction.

Experiments with all studied base catalysts revealed that this new domino reaction is moisture-, air-, and light-insensitive. Another important aspect of the reaction is the control over the chemoselectivity through the input of a certain electrophile (e.g., hydrazone **1** vs. aldehyde **5a**) or catalyst (Figure 3, see also the Supporting Information).

Further systematic investigation of different commercially available organic bases and several imidazole derivatives (see the Supporting Information) demonstrated that simple unsubstituted imidazole was still the best choice. Therefore, and with the imidazole as a catalyst, different aldehydes were then evaluated as substrates and the results are summarized in Figure 4.

### Substrate scope

The use of propanal **5b** as a substrate gave the corresponding products **3b** and **4b** in 11:1 ratio. The diastereomeric ratio (d.r.) of the major product **3b** was 38:62 (*anti*-**3b**/*syn*-**3b**). Interestingly, the diastereomer *syn*-**3a**, which was formed only in trace amounts (d.r. > 99:1, *anti*-**3a**/*syn*-**3a**) using phenylethanal **5a**, was generated as a major diastereomer (*syn*-**3b**) using propanal **5b** as an aldehyde. The detailed X-ray and NMR studies on relative configuration assignment of the obtained diastereomers will be discussed later in this paper.

Next, several arylethanal **5c–5j** were evaluated as substrates. Overall yields are 40–59% for six steps, and **3/4** ratios ranging from 2:1 to 7:1 were obtained (Figure 4). Intriguingly,

the highly functionalized racemic isoquinuclidine molecules **3c–j**, which were the main products in all cases, were isolated with diastereoselectivities of up to more than 99:1 (similar to **3a**). It is amazing that all four stereogenic centers (one quaternary and three tertiary) can be controlled highly diastereoselectively in this multi-step reaction using simply achiral imidazole as a catalyst.

We next turned our attention to artemisinin-derived aldehydes as substrates. Since the seminal discovery in 1972 of artemisinin (natural 1,2,4-trioxane sesquiterpene) from *Artemisia annua* L., by Youyou Tu (Nobel Prize 2015),<sup>[14]</sup> diverse varieties of artemisinin-derived dimers and hybrids have been synthesized. Natural product hybrid molecules<sup>[15]</sup> often possess strikingly improved or new biological activities compared with those of their parent compounds, as reported by our group and others on examples of different highly potent artemisinin-derived hybrids with antimalarial, antiviral, and anticancer activities.<sup>[16]</sup>

Thus, predicting the potential of our new transformation to structurally diverse and complex scaffolds of value to medicinal chemistry, we next prepared artemisinin-derived hybrids. We carried out two reactions of enantiomerically pure artemisinin-based aldehydes **5k** and **5l** with malononitrile **2**, respectively, in the presence of imidazole (15 mol%). Delightfully, new artemisinin-derived hybrids **3k** and **4k** were synthesized in 52% overall yield, 5:1 ratio and hybrids **3l** and **4l** were synthesized in 38% overall yield. A 3:1 ratio of corresponding products were formed (Figure 4).

The diastereomeric ratios in the isoquinuclidine heterocyclic subunits of the major products **3k** and **3l** were determined by <sup>1</sup>H NMR spectroscopy as 75:25 (*anti*-**3k**/*syn*-**3k**) and 90:10 (*anti*-**3l**/*syn*-**3l**), respectively.

The obtained hybrids **3k**, **3l**, **4k**, and **4l** are currently under biological investigations. The antiviral activities of the selected new molecules **3l** and **4l** were already assessed in vitro. Remarkably, hybrids **3l** and **4l** display superior potency against HCMV (human cytomegalovirus) (EC<sub>50</sub> of (0.071 ± 0.002) μM and (0.260 ± 0.008) μM, respectively) compared with that of their parent compound artemisinin (EC<sub>50</sub> > 10 μM<sup>[30,31]</sup>) and are even more active than clinically used antiviral agent ganciclovir

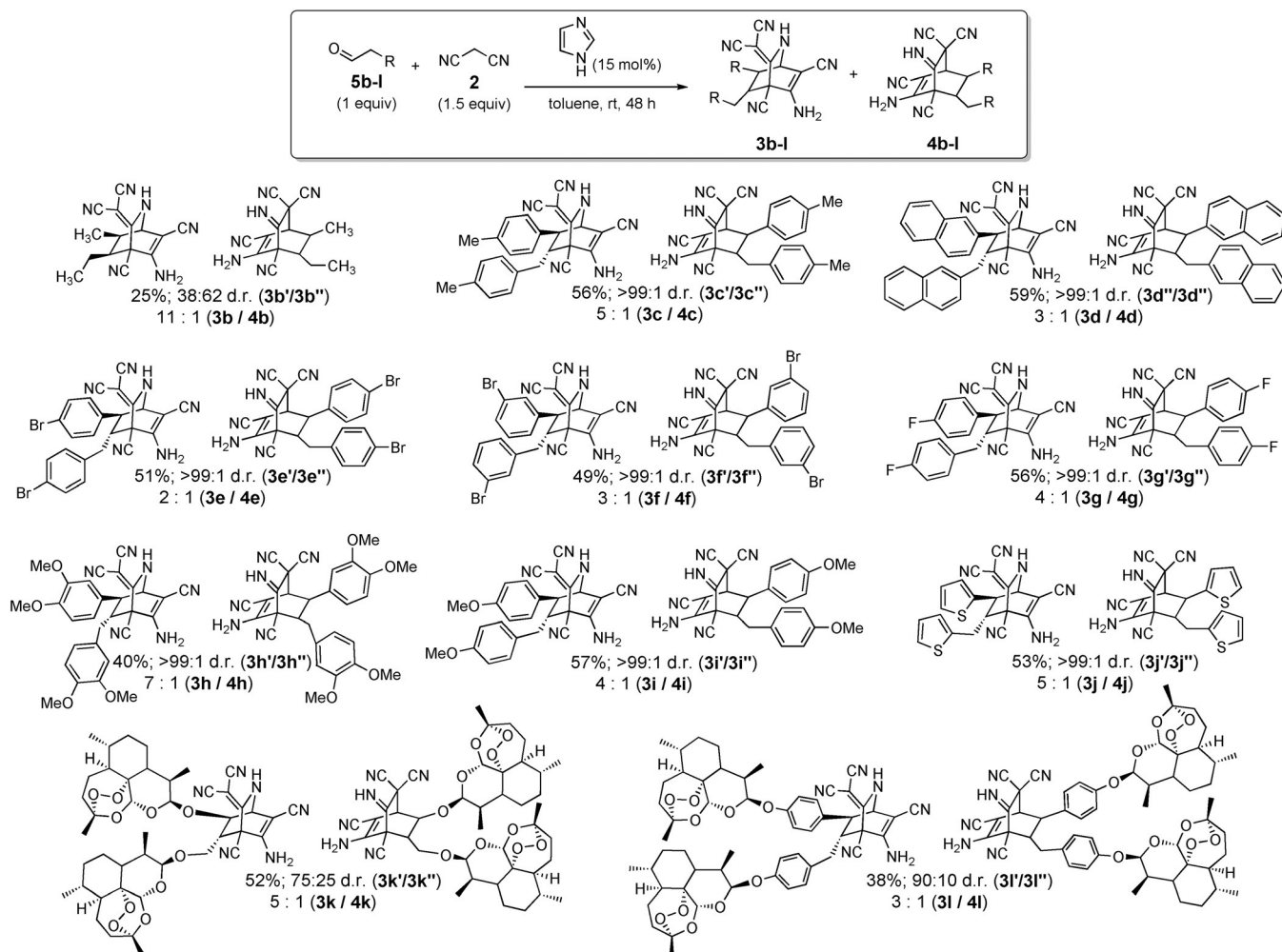


**Figure 4.** Substrate scope includes various aldehydes **5b–5l**. Reported yields were isolated yields of products, sum of **3** and **4**. Ratio **3/4** and d.r. were determined by  $^1\text{H}$  NMR analysis of the product mixture after a single column, see the Supporting Information for more details.

( $\text{EC}_{50}$  of  $(2.6 \pm 0.5) \mu\text{M}$ <sup>[30,31]</sup>). The detailed results of the biological studies will be reported elsewhere.

Further demonstration of the immense potential of this six-step domino reaction to deliver, in a single operation, new libraries of artemisinin-derived hybrid molecules and hybrids of different other bioactive compounds with antiviral, anticancer and antimalarial properties is currently underway in our laboratory.

#### X-ray and NMR studies on the stereochemistry of new products

The structures and relative stereochemistry of the isoquinuclidines **anti-3a'** (formed as a single diastereomer (d.r. > 99:1) from phenylethanal **5a**) and **anti-3b'** (formed from propanal **5b** as a minor diastereomer, d.r. 38:62), were confirmed by X-ray analysis of single crystals obtained by slow evaporation of the solvent (Figure 5).<sup>[17]</sup>

As discussed above, compound **3b** (R=CH<sub>3</sub>, see Figure 4) was obtained as a mixture of two diastereomers **anti-3b'**/**syn-3b''** in a 38:62 ratio. Whereas the structure of minor diastereomer **anti-3b'** was determined by X-ray analysis (Figure 5), the

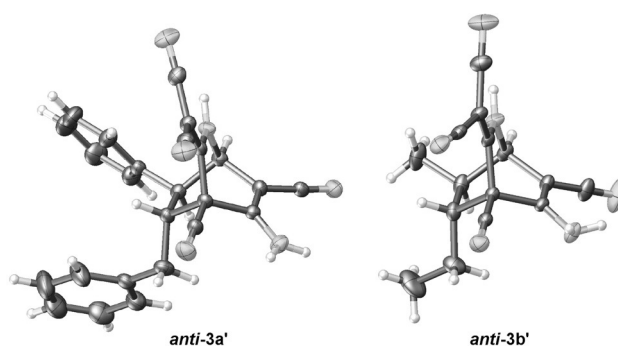


**Figure 5.** ORTEP view of molecular structure of polysubstituted isoquinuclidines **anti-3a'** and **anti-3b'**.

major diastereomer **syn-3b''** was subjected to an extensive NMR analysis, in particular with respect of the *exo/endo* assignment of the methyl and ethyl group. Apart from standard  $^1\text{H}$ - and  $^{13}\text{C}$ -measurements, methods employed were HMQC, HMBC, COLOC, COSY, NOESY, and  $^1\text{H}$ ,  $^{13}\text{C}$ -HOESY. For convenience, we employ the numbering shown in Figure 6A as is suggested by the CSEARCH/NMRPredict software.<sup>[18]</sup> Some selected NMR-findings will be presented here.

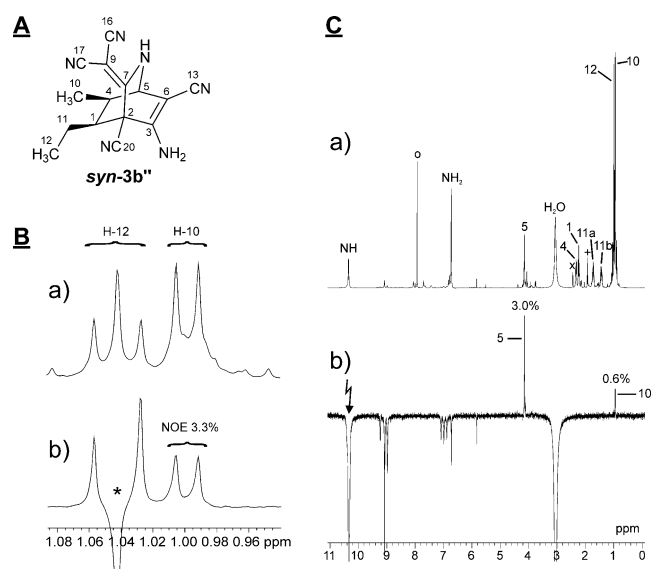


**Figure 6.** A) Numbering of **syn-3b'** as automatically suggested by the NMRpredict software and as is employed for the depicted/described NMR spectra; B)  $^1\text{H}$  NMR spectrum (500 MHz) of **syn-3b'**, magnified signals of H-12 (ethyl- $\text{CH}_3$ ) and H-10 (methyl) in  $[\text{D}_6]\text{DMSO}/\text{CD}_3\text{CN}$  1:2, RT; a) normal  $^1\text{H}$ -spectrum; b) DPFGE-NOE spectrum under irradiation of H-11b (one of the diastereotopic  $\text{CH}_2$ -protons). The percentage number is relative to the intensity of the irradiated signal = -100%. [\*] denotes a selective population transfer (SPT) effect from vicinal coupling. Measuring time for the NOE spectrum: 5 h; C)  $^1\text{H}$  NMR spectrum (500 MHz) of **syn-3b'** in  $[\text{D}_6]\text{DMSO}/\text{CD}_3\text{CN}$  1:2, RT a) normal  $^1\text{H}$ -spectrum with assignments according to A; [o] =  $\text{CHCl}_3$  (from synthesis/workup); [x] = residual solvent signal ( $[\text{D}_6]\text{DMSO}$ ); [+] = residual solvent signal ( $\text{CD}_3\text{CN}$ ); b) DPFGE-NOE spectrum under irradiation of the NH signal. Negative signals are due to chemical exchange with other acidic protons from isomerization/decomposition products. Percentage numbers of positive NOE signals at H-5 and H-10 are relative to the integral sum of all negative signals = -100%. Mixing time 0.5 s, measuring time 22 h.

In a DPFGE-NOE experiment, the  $^1\text{H}$ -signal of H-11b was irradiated (one of the two diastereotopic  $\text{CH}_2$ -protons). An intense NOE of 3.3% to H-10 (the three protons of the neighboring Me-group) has been observed (Figure 6B). This shows the ethyl and methyl groups to be in *syn* arrangement. A further proof of the *syn* position of Et and Me comes from irradiation of H-4: only very weak NOEs are found to the  $\text{CH}_2$  protons H-11a and H-11b (not depicted).

In a further DPFGE-NOE experiment, the NH-signal at  $\delta = 10.39$  was irradiated (Figure 6C). Negative signals in Figure 6C(b) indicate chemical exchange with other acidic protons present in the molecule and in solution. Besides the expected exchange of the NH proton with the  $\text{NH}_2$  protons, there is further exchange with the  $\text{H}_2\text{O}$  protons as well as with acidic protons from isomerization/decomposition products. However, positive signals in Figure 6C(b) indicate NOEs. An expected strong (3.0%) NOE is found to the close-by proton H-5. Furthermore, a moderately intense NOE (0.6%) is found to H-10 (Me-protons). Noteworthy, not even a weak NOE is found for H-4. Clearly, this indicates the methyl group H-10 to be in *exo* position. Along with the above finding that the ethyl and methyl group are *syn*, we conclude that in this particular diastereomer **3b'** the ethyl and methyl groups both are *exo*.

## Mechanism based on mass spectrometric studies

Domino reactions, a concept pioneered by Tietze, represent a highly promising route for the preparation of complex molecules and pharmaceutically important compounds.<sup>[19]</sup> Multi-step domino reactions involving organocatalysis are among the most recent, elegant, sustainable and economically attractive methods allowing to form complex molecular scaffolds from simple components.<sup>[20]</sup>

We next hypothesized on the mechanism for our new chemodivergent domino reaction of phenylethanal **5a** with malononitrile **2** based on EI- and APPI-MS studies (Figure 7, see also the Supporting Information). In the presence of imidazole under the optimized reaction conditions, we observed signals at  $m/z$  168  $[M]^+$  (Knoevenagel product),  $m/z$  337  $[M+H]^+$  (dimerization product), and  $m/z$  403  $[M+H]^+$ , which corresponds to the products of all subsequent steps (interestingly, the molecular weight of all product intermediates and the final products is 402).

A plausible reaction pathway of the formation of isoquinuclidine **3a** and carbobicyclic **4a** from phenylacetaldehyde **5a** and malononitrile **2** through a domino reaction is illustrated in Figure 7. The reaction either proceeds through the six-step sequence of a Knoevenagel/dimerization/intermolecular addition/intramolecular aza-Michael/intramolecular addition/tautomerization (product **3a** formation), or, through the six-step sequence of a Knoevenagel/dimerization/Michael/intramolecular addition 1/tautomerization/intramolecular addition 2 (product **4a** formation). The **3a/4a** product ratio might be subject to thermodynamic control, due to the potentially greater thermodynamic stability of **3a** versus **4a** (see below). We hitherto assumed here that imidazole acts as specific base catalyst. Alternatively, the catalyst could be involved here as a general base catalyst in the intermolecular addition (**6**→**7**). In contrast, the Michael reaction step (**6**→**8**) in the formation of **4a** is most likely configuration determining and apparently the product ratio becomes predominantly kinetically controlled here.

This chemodivergent domino reaction could in principle proceed also through seven-steps involving Michael and Knoevenagel reactions instead of the dimerization step of the initial Knoevenagel product. In both cases, there is a system of two interacting simple molecules **2** and **5a** that link together into larger structures, allowing a consecutive series of further steps (domino reactions), leading to complex bicyclic nitrogen-containing molecules **3a** and **4a**.

## DFT studies on the mechanism

To shed some more light on the chemoselectivity, and, in particular, to understand the influence of dispersion interactions<sup>[21]</sup> in the imidazole-catalyzed transformation, mechanistic investigations have been performed using DFT methods in conjunction with semiempirical van der Waals interactions. Computational details are provided in the Supporting Information.

First, we note that product **3a** is more stable than **4a** by  $\approx 12 \text{ kcal mol}^{-1}$  (Gibbs energy), that is, from thermodynamics alone one would expect that molecule **4a** is formed in an only

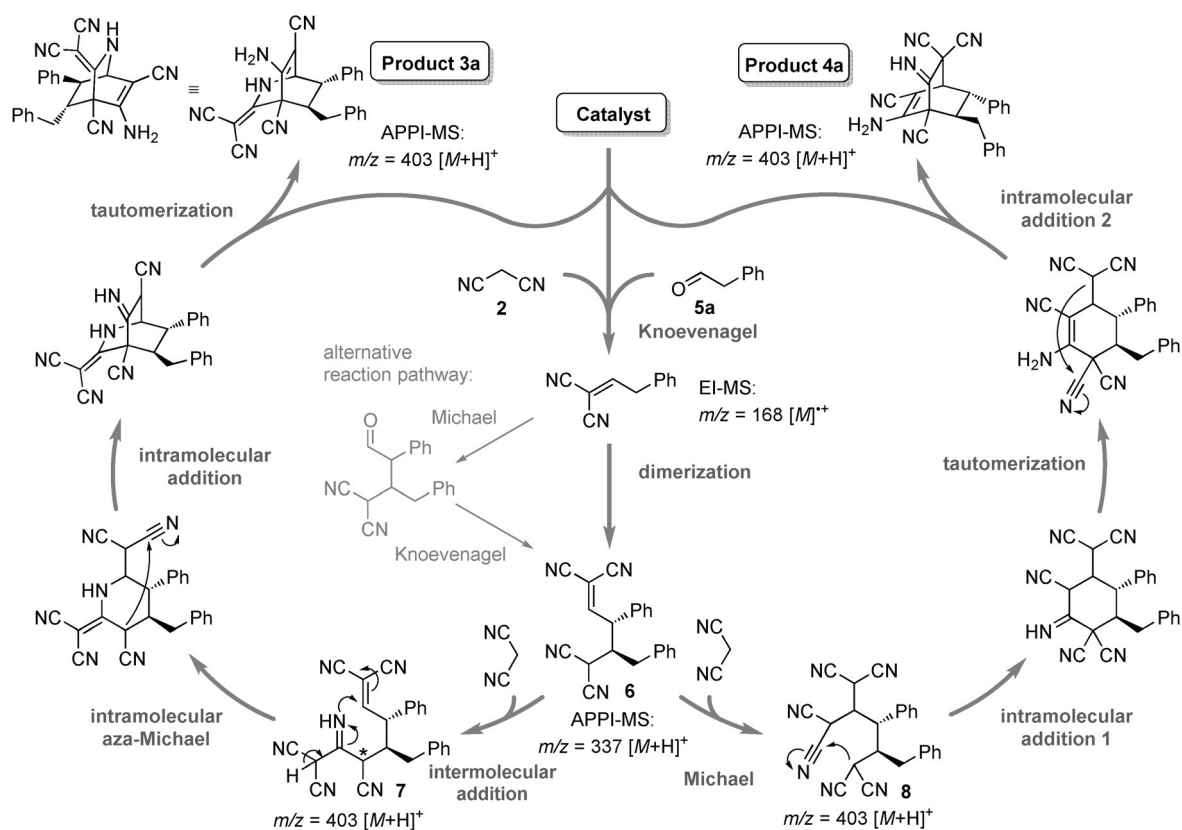


Figure 7. Proposed mechanism of the chemodivergent multi-step domino reaction leading to compounds **3a** and **4a**.

negligible amount at room temperature (Figure 8). However, as this is not the case (although **3a** is usually the more dominant product) with imidazole as catalyst, the reaction cannot be controlled alone by the overall thermodynamics.

According to our presumed mechanism, the reaction of the intermediate **6** with malononitrile forms the branching point between the reactions leading to **3a** and **4a**, and may pre-determine the observed product ratio. Therefore, we studied this “chemoselective” step in more detail. Since the molecules **6**, **7**, and **8** are very flexible, various conformers, as well as two diastereomers in case of **7** (*RRS* and *RRR*), have been taken into account (see the Supporting Information for details). Overall, we have computed 103 different conformers. The relative Gibbs energies of the six most stable conformers for each of the mentioned species (including the products **3a** and **4a**) and the optimized structures of the most stable species are shown in Figure 8.

The reaction pathways from **6** to **7**, or **8**, respectively, are both endergonic partly due to entropy effects (by reduction of the number of molecules) in addition to enthalpy effects, but the nucleophilic addition (**6**→**7**), which leads to product **3a**, is favored by 4.7 kcal mol<sup>-1</sup> versus the Michael addition (**6**→**8**). To obtain some information about the kinetics of this step, we calculated exemplary transition states (TS) for both pathways with imidazole as model catalyst (see the Supporting Information for details). The results are depicted in Figure 9.

The reactants **6** (in form of the conformer leading to the lowest TS), malononitrile and imidazole, first make up a reac-

tant complex with deprotonated malononitrile and the imidazolium cation. Via a transition state structure, this reactant

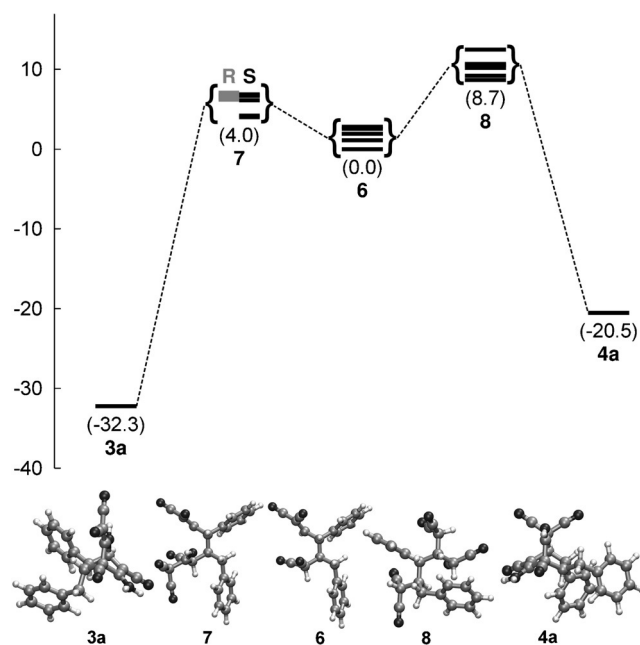
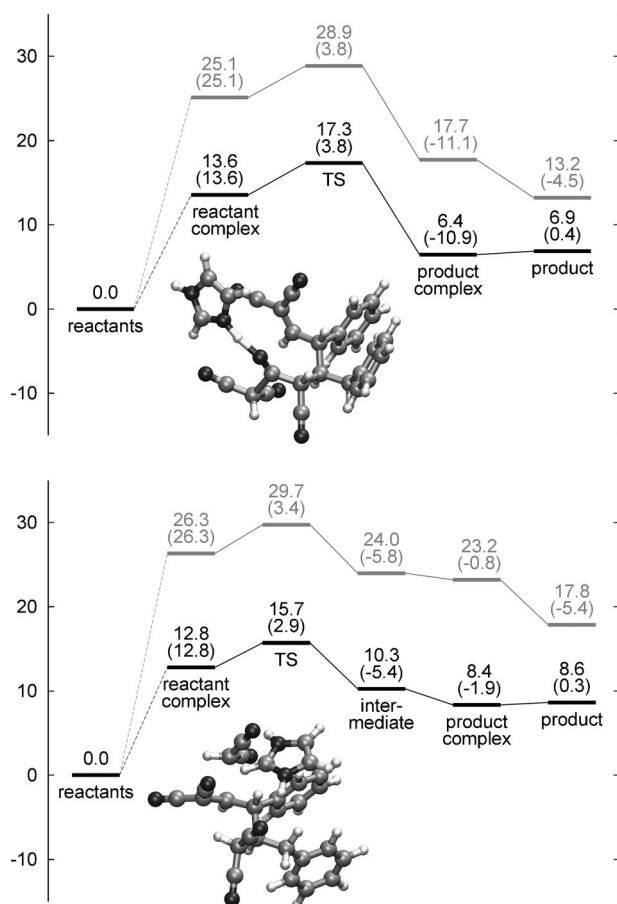


Figure 8. Free energies (in kcal mol<sup>-1</sup>) of the most stable conformers relative to the most stable conformer of **6**. In case of the addition product **7** the *R* and *S* configurations on the C atom marked by an asterisk in Figure 7 were considered.



**Figure 9.** Reaction profiles of the nucleophilic addition reaction (upper graph) and Michael addition (lower graph), catalyzed by imidazole, respectively. Free energies (in  $\text{kcal mol}^{-1}$ ) are relative to the reactants (most stable conformer **6** + imidazole + malononitrile). The free energies are also given relative to the reactant level or the previous species (in parenthesis). The black line represents the profile with van der Waals corrections, whereas the gray line represents the profile without. Additionally, the structures of the respective transition states are shown.

complex leads directly to the complex of the product **7** and imidazole in case of the nucleophilic addition. In the case of the Michael addition, the corresponding transition state structure leads to an intermediate complex of the deprotonated product **8** and imidazolium, which then yields a complex of the Michael product and imidazole after a reprotonation step.

The activation energy for the nucleophilic addition reaction was found to be  $3.8 \text{ kcal mol}^{-1}$  relative to the reactant complex. The reaction leading from the reactant complex to the product complex is exergonic with a reaction energy of  $-7.2 \text{ kcal mol}^{-1}$ . The Michael reaction features a somewhat lower activation energy of  $2.9 \text{ kcal mol}^{-1}$  relative to the reactant complex and a reaction free energy of  $-4.4 \text{ kcal mol}^{-1}$ . The reaction profiles and the optimized structure of the TSs are shown in Figure 9. Thus, the Michael reaction leading to **4a** seems to be faster ( $\Delta\Delta G^\ddagger = 0.9 \text{ kcal mol}^{-1}$ ), whereas the addition reaction leading to **3a** is thermodynamically favored by  $2.0 \text{ kcal mol}^{-1}$ .

We note, however, that the difference in the activation barrier is rather small, and the reaction energies are positive for

both competing steps (see Figure 9), and the addition itself may be regarded therefore as reversible at room temperature (also in light of the moderate activation barriers). This means that the observed chemoselectivity of the domino reaction may also be influenced by the following reaction steps in addition to the activation barriers of the investigated “chemoselective” step. However, a comprehensive theoretical investigation of all reaction steps in Figure 7 is beyond the scope of the present study. Furthermore, solvent effects on reaction energies and activation barriers might also play a role.

Our final point of interest was whether dispersion interactions have a special effect on the kinetics and thermodynamics of the reaction. For this purpose we calculated the free energies without dispersion interactions (see the Supporting Information for details).

If dispersion interactions are neglected, the Michael product **8** becomes more destabilized with respect to the addition product **7**. Considering the final products, compound **3a** is  $5.1 \text{ kcal mol}^{-1}$  and **4a** is  $6.8 \text{ kcal mol}^{-1}$  less stable without dispersion interactions. It seems that dispersion interactions stabilize the reaction path towards **4a** more than the pathway towards **3a** and therefore may decrease also the ratio of **3a/4a**. Furthermore, the free energies of the intermediates of the imidazole-catalyzed reaction are lowered relative to the energies of the reactants by dispersion interactions. This energetic lowering of the reaction intermediates is stronger in the case of the Michael reaction than in the case of the nucleophilic addition. The Michael reaction therefore seems to be favored by dispersion interactions also kinetically.

## Conclusion

We have demonstrated here an unexpected formation of complex molecular architectures (bicyclic nitrogen-containing molecules **3** and **4** of importance for medicinal research) from two strikingly simple components. The unprecedented six-step imidazole-catalyzed domino reaction enables a convenient, modular, and efficient direct route to biologically active isoquinuclidine ring systems and their isomeric carbobicycles using simple aldehydes and commodity malononitrile as starting materials. This obviates the need of work-up and purification steps for the synthesis of complex target compounds, leading to a reduction of costs and materials, and makes the presented synthetic strategy sustainable, straightforward, atom economical, and environmentally friendly. The chemoselectivity seems to depend on small differences in transition state and reaction energies of the branching step. Furthermore, the chemoselectivity may also be influenced by the energetics of subsequent reactions steps. Dispersion interactions lower the energies of the intermediates and products of the branching step relative to the reactants, which may conceivably result in higher yields. In addition, we found that the two distinct reaction pathways and corresponding product ratios of **3** versus **4** can be controlled by the applied electrophiles or catalysts. This might allow us to shift the chemoselectivity to either **3** or **4** at will.

Finally, the first artemisinin-isoquinuclidine and artemisinin-carbobicyclic hybrid molecules with strong antiviral activities

(EC<sub>50</sub> up to 0.071 μM for HCMV) could easily be prepared using this six-step domino reaction. Further efforts to diversify/apply this new six-step domino reaction to the synthesis of new target structures as well as new libraries of natural product hybrids with potential antiviral, anticancer, and antimalarial activities is currently underway in our laboratory.

## Experimental Section

### Materials

For details of the synthetic procedures and <sup>1</sup>H, <sup>13</sup>C NMR, MS spectra of compounds in this manuscript, see the Supporting Information.

### General procedure for the domino reaction

Aldehyde (0.24 mmol), malononitrile (24 mg, 0.36 mmol) and the appropriate catalyst (0.018 mmol) were dissolved in toluene (C<sub>aldehyde</sub> = 0.48 mol L<sup>-1</sup>). The reaction mixture was stirred at room temperature until malononitrile was completely consumed. The reaction was stopped by evaporating the solvent. The crude product was purified by silica gel column chromatography (hexane/ethyl acetate = 5:1 to 3:1).

### Acknowledgements

The authors gratefully acknowledge the financial support by grants from Deutsche Forschungsgemeinschaft TS 87/15-1 and Priority Programme "Control of London Dispersion Interactions in Molecular Chemistry" (SPP 1807): TS 87/17-1 and GO 523/16-1. We thank Prof. M. Marschall and Dr. C. Hutterer (Institute for Clinical and Molecular Virology, FAU) for biological studies on the new compounds **3I** and **4I**. The authors thank Aysun Çapcı Karagöz for the preparation of aldehyde **5k** and preliminary studies on domino reaction using this aldehyde and also acknowledge the synthesis of aldehyde **5I** by Dr. Hitesh Jalani. We thank the Interdisciplinary Center for Molecular Materials (ICMM) for research support and the Elite Network of Bavaria for a doctoral research fellowship for Christina M. Bock.

**Keywords:** antiviral agents • density functional calculations • domino reaction • organocatalysis • medicinal chemistry

- [1] a) M. E. Kuehne, L. He, P. A. Jokiel, C. J. Pace, M. W. Fleck, I. M. Maison-neuve, S. D. Glick, J. M. Bidlack, *J. Med. Chem.* **2003**, *46*, 2716–2730; b) Z. Ye, L. Guo, K. J. Barakat, P. G. Pollard, B. L. Palucki, I. K. Sebbat, R. K. Bakshi, R. Tang, R. N. Kalyani, A. Vongs, A. S. Chen, H. Y. Chen, C. I. Rosenblum, T. MacNeil, D. H. Weinberg, Q. Peng, C. Tamvakopoulos, R. R. Miller, R. A. Stearns, D. E. Cashen, W. J. Martin, J. M. Metzger, A. M. Strack, D. E. MacIntyre, L. H. T. Van der Ploeg, A. A. Patchett, M. J. Wyv-ratt, R. P. Nargund, *Bioorg. Med. Chem. Lett.* **2005**, *15*, 3501–3505; c) M. O. Faruk Khan, M. S. Levi, B. L. Tekwani, N. H. Wilson, R. F. Borne, *Bioorg. Med. Chem.* **2007**, *15*, 3919–3925.
- [2] S. L. T. Cappendijk, M. R. Dzoljic, *Eur. J. Pharmacol.* **1993**, *241*, 261–265.
- [3] C. B. Page, A. R. Pinder, *J. Chem. Soc.* **1964**, 4811–4816.
- [4] J. C. Delorenzi, M. Attias, C. R. Gattass, M. Andrade, C. Rezende, A. da Cunha Pinto, A. T. Henriques, D. C. Bou-Habib, E. M. B. Saraiva, *Antimi-crob. Agents Chemother.* **2001**, *45*, 1349–1354.
- [5] a) K. K. C. Liu, S. M. Sakya, C. J. O'Donnell, A. C. Flick, J. Li, *Bioorg. Med. Chem.* **2011**, *19*, 1136–1154; b) G. L. Patrick, *An Introduction to Drug Synthesis*, Oxford University Press, **2015**.
- [6] a) W. Seebacher, C. Schlapper, R. Brun, M. Kaiser, R. Saf, R. Weis, *Eur. J. Pharm. Sci.* **2005**, *24*, 281–289; b) W. Seebacher, C. Schlapper, R. Brun, M. Kaiser, R. Saf, R. Weis, *Eur. J. Med. Chem.* **2006**, *41*, 970–977.
- [7] a) M. Igarashi, Y. Nakano, K. Takezawa, T. Watanabe, S. Sato, *Synthesis* **1987**, 1987, 68–70; b) Y. Nakano, W.-Y. Shi, Y. Nishii, M. Igarashi, *J. Hetero-cycl. Chem.* **1999**, *36*, 33–40; c) Y. Nakano, Y. Kaneko, W. A. Fen, *Hetero-cycles* **1999**, *51*, 169–177; d) N. Mahajan, V. Gupta, P. Kotwal, A. S. Pannu, T. K. Razdan, *J. Chem. Crystallogr.* **2011**, *41*, 552–556; e) Y. Kohari, Y. Okuyama, E. Kwon, T. Furuyama, N. Kobayashi, T. Otuki, J. Kumagai, C. Seki, K. Uwai, G. Dai, T. Iwasa, H. Nakano, *J. Org. Chem.* **2014**, *79*, 9500–9511.
- [8] M. Rueping, C. Azap, *Angew. Chem. Int. Ed.* **2006**, *45*, 7832–7835; *Angew. Chem.* **2006**, *118*, 7996–7999.
- [9] H. Yang, R. G. Carter, *J. Org. Chem.* **2009**, *74*, 5151–5156.
- [10] H. Nakano, K. Osone, M. Takeshita, E. Kwon, C. Seki, H. Matsuyama, N. Takano, Y. Kohari, *Chem. Commun.* **2010**, *46*, 4827–4829.
- [11] V. Thornqvist, S. Manner, M. Wingstrand, T. Frejd, *J. Org. Chem.* **2005**, *70*, 8609–8612.
- [12] D. Schinzer, M. Kalesse, *Tetrahedron Lett.* **1991**, *32*, 4691–4694.
- [13] a) D. A. Yalalov, S. B. Tsogoeva, T. E. Shubina, I. M. Martynova, T. Clark, *Angew. Chem. Int. Ed.* **2008**, *47*, 6624–6628; *Angew. Chem.* **2008**, *120*, 6726–6730; b) S. B. Tsogoeva, S. Wei, M. Freund, M. Mauksch, *Angew. Chem. Int. Ed.* **2009**, *48*, 590–594; *Angew. Chem.* **2009**, *121*, 598–602.
- [14] Y. Tu, *Nat. Med.* **2011**, *17*, 1217–1220.
- [15] a) L. F. Tietze, H. P. Bell, S. Chandrasekhar, *Angew. Chem. Int. Ed.* **2003**, *42*, 3996–4028; *Angew. Chem.* **2003**, *115*, 4128–4160; b) B. Meunier, *Acc. Chem. Res.* **2008**, *41*, 69–77; c) S. B. Tsogoeva, *Mini-Rev. Med. Chem.* **2010**, *10*, 773–793.
- [16] a) C. Horwedel, S. B. Tsogoeva, S. Wei, T. Efferth, *J. Med. Chem.* **2010**, *53*, 4842–4848; b) C. Reiter, A. Herrmann, A. Çapcı, T. Efferth, S. B. Tsogoeva, *Bioorg. Med. Chem.* **2012**, *20*, 5637–5641; c) C. Reiter, A. Çapcı Karagöz, T. Fröhlich, V. Klein, M. Zeino, K. Viertel, J. Held, B. Mordmüller, S. Emir-dağ Öztürk, H. Anil, T. Efferth, S. B. Tsogoeva, *Eur. J. Med. Chem.* **2014**, *75*, 403–412; Öztürk, H. Anil, T. Efferth, S. B. Tsogoeva, *Eur. J. Med. Chem.* **2014**, *75*, 403–412; d) C. Reiter, T. Fröhlich, M. Zeino, M. Marschall, H. Bahsi, M. Leidenberger, O. Friedrich, B. Kappes, F. Hampel, T. Efferth, S. B. Tsogoeva, *Eur. J. Med. Chem.* **2015**, *97*, 164–172; e) C. Reiter, T. Fröhlich, L. Gruber, C. Hutterer, M. Marschall, C. Voigtländer, O. Friedrich, B. Kappes, T. Efferth, S. B. Tsogoeva, *Bioorg. Med. Chem.* **2015**, *23*, 5452–5458.
- [17] CCDC 991547 (**3a'**), 1435950 (**3b'**) contain the supplementary crystallo-graphic data for this paper. These data are provided free of charge by The Cambridge Crystallographic Data Centre.
- [18] CSEARCH/NMRpredict software package, W. Robien, University of Vienna, Austria; <http://nmrpredict.orc.univie.ac.at/> last viewed October 24, 2015.
- [19] a) L. F. Tietze, *Chem. Rev.* **1996**, *96*, 115–136; b) H.-C. Guo, J.-A. Ma, *Angew. Chem. Int. Ed.* **2006**, *45*, 354–366; *Angew. Chem.* **2006**, *118*, 362–375; c) L. F. Tietze, G. Brasche, K. M. Gericke, *Domino Reactions in Organic Synthesis*, Wiley-VCH, Weinheim, **2006**; d) H. Pellissier, *Tetrahe-dron* **2006**, *62*, 1619–1665; e) H. Pellissier, *Tetrahedron* **2006**, *62*, 2143–2173; f) K. C. Nicolaou, D. J. Edmonds, P. G. Bulger, *Angew. Chem. Int. Ed.* **2006**, *45*, 7134–7186; *Angew. Chem.* **2006**, *118*, 7292–7344; g) C. J. Chapman, C. G. Frost, *Synthesis* **2007**, 1–21; h) D. Enders, C. Grondal, M. R. M. Hüttl, *Angew. Chem. Int. Ed.* **2007**, *46*, 1570–1581; *Angew. Chem.* **2007**, *119*, 1590–1601; i) C. Vaxelaire, P. Winter, M. Christmann, *Angew. Chem. Int. Ed.* **2011**, *50*, 3605–3607; *Angew. Chem.* **2011**, *123*, 3685–3687; j) Ł. Albrecht, H. Jiang, K. A. Jørgensen, *Angew. Chem. Int. Ed.* **2011**, *50*, 8492–8509; *Angew. Chem.* **2011**, *123*, 8642–8660; k) L. F. Tietze, *Domino Reactions: Concepts for Efficient Organic Synthesis*, Wiley-VCH, Weinheim, **2014**.
- [20] a) R. Marcia de Figueiredo, M. Christmann, *Eur. J. Org. Chem.* **2007**, 2575–2600; b) C. Grondal, M. Jeanty, D. Enders, *Nat. Chem.* **2010**, *2*, 167–178; c) E. Marqués-López, R. P. Herrera, M. Christmann, *Nat. Prod. Rep.* **2010**, *27*, 1138–1167; d) M. Rueping, J. Dufour, F. R. Schoepke, *Green Chem.* **2011**, *13*, 1084–1105; e) D. Enders, M. R. M. Hüttl, C. Grondal, G. Raabe, *Nature* **2006**, *441*, 861–863; f) A. Carlone, S. Cabrera, M. Marigo, K. A. Jørgensen, *Angew. Chem. Int. Ed.* **2007**, *46*, 1101–1104; *Angew. Chem.* **2007**, *119*, 1119–1122; g) D. Enders, M. R. M. Hüttl, G. Raabe, J. W. Bats, *Adv. Synth. Catal.* **2008**, *350*, 267–279; h) H. Ishikawa, T. Suzuki, Y. Hayashi, *Angew. Chem. Int. Ed.* **2009**, *48*, 1304–1307; *Angew.*



- Chem.* **2009**, *121*, 1330–1333; i) L.-Y. Wu, G. Bencivenni, M. Mancinelli, A. Mazzanti, G. Bartoli, P. Melchiorre, *Angew. Chem. Int. Ed.* **2009**, *48*, 7196–7199; *Angew. Chem.* **2009**, *121*, 7332–7335; j) H. Ishikawa, T. Suzuki, H. Orita, T. Uchimaru, Y. Hayashi, *Chem. Eur. J.* **2010**, *16*, 12616–12626; k) K. Jiang, Z.-J. Jia, S. Chen, L. Wu, Y.-C. Chen, *Chem. Eur. J.* **2010**, *16*, 2852–2856; l) B.-C. Hong, P. Kotame, C.-W. Tsai, J.-H. Liao, *Org. Lett.* **2010**, *12*, 776–779; m) D. Enders, R. Krüll, W. Bettray, *Synthesis* **2010**, *2010*, 567–572; n) D. Enders, C. Wang, M. Mukanova, A. Greb, *Chem. Commun.* **2010**, *46*, 2447–2449; o) T. Urushima, D. Sakamoto, H. Ishikawa, Y. Hayashi, *Org. Lett.* **2010**, *12*, 4588–4591; p) K. Jiang, Z.-J. Jia, X. Yin, L. Wu, Y.-C. Chen, *Org. Lett.* **2010**, *12*, 2766–2769; q) H. Ishikawa, M. Honma, Y. Hayashi, *Angew. Chem. Int. Ed.* **2011**, *50*, 2824–2827; *Angew. Chem.* **2011**, *123*, 2876–2879; r) G. Dickmeiss, K. L. Jensen, D. Worgull, P. T. Franke, K. A. Jørgensen, *Angew. Chem. Int. Ed.* **2011**, *50*, 1580–1583; *Angew. Chem.* **2011**, *123*, 1618–1621; s) M. Rueping, K. Haack, W. leaw-suwan, H. Sunden, M. Blanco, F. R. Schoepke, *Chem. Commun.* **2011**, *47*, 3828–3830.
- [21] a) D. Seebach, U. Grošelj, W. B. Schweizer, S. Grimme, C. Mück-Lichtenfeld, *Helv. Chim. Acta* **2010**, *93*, 1–16; b) C. Reiter, S. López-Molina, B. Schmid, C. Neiss, A. Görling, S. B. Tsogoeva, *ChemCatChem* **2014**, *6*, 1324–1332; c) A. Armstrong, R. A. Boto, P. Dingwall, J. Contreras-Garcia, M. J. Harvey, N. J. Mason, H. S. Rzepa, *Chem. Sci.* **2014**, *5*, 2057–2071.

Received: November 28, 2015

Published online on February 26, 2016